Journal of Advanced Research 27 (2021) 31–40

Contents lists available at ScienceDirect

Journal of Advanced Research

journal homepage: www.elsevier.com/locate/jare

Hippocampal ornithine decarboxylase/spermidine pathway mediates H_2S-alleviated cognitive impairment in diabetic rats: Involving enhancment of hippocampal autophagic flux

Xuan Kang [a,b,1], Cheng Li [c,d,1], Yan Xie [d], Ling-Li He [d], Fan Xiao [b], Ke-Bin Zhan [d,*], Yi-Yun Tang [b], Xiang Li [e], Xiao-Qing Tang [a,b,*]

[a] Institute of Neurology, The First Affiliated Hospital, University of South China, Hengyang 421001, Hunan, PR China
[b] Institute of Neuroscience, Hengyang Medical College, University of South China, Hengyang 421001, Hunan, PR China
[c] Department of Emergency Affiliated Nanhua Hospital, University of South China, Hengyang 421001, Hunan, PR China
[d] Department of Neurology, The Second Affiliated Hospital, University of South China, Hengyang 421001, Hunan, PR China
[e] Department of Anesthesiology, The First Affiliated Hospital, University of South China, Hengyang 421001, Hunan, PR China

GRAPHICAL ABSTRACT

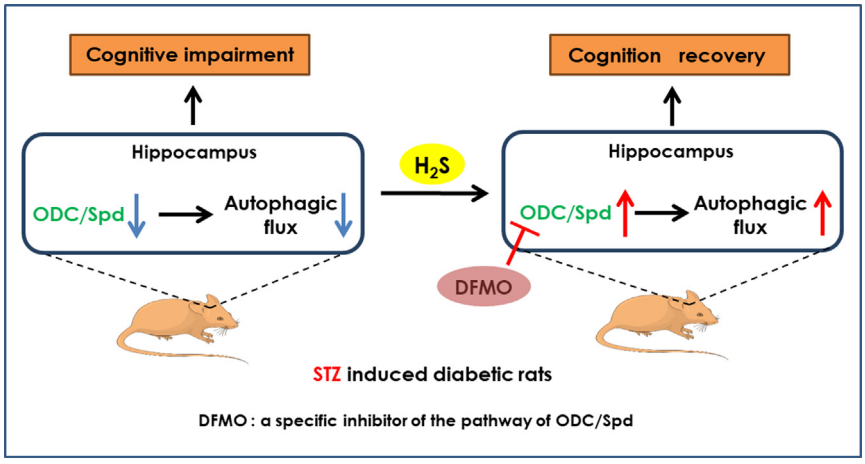

ARTICLE INFO

Article history:
Received 23 February 2020
Revised 14 May 2020
Accepted 9 June 2020
Available online 12 June 2020

Keywords:
Autophagic flux
Cognitive impairment

ABSTRACT

Introduction: We have previously demonstrated the antagonistic role of hydrogen sulfide (H2S) in the cognitive dysfunction of streptozotocin (STZ)-induced diabetic rats. It has been confirmed that the impaired hippocampal autophagic flux has a key role in the pathogenesis of cognitive impairment and that ornithine decarboxylase (ODC)/spermidine (Spd) pathway plays an important role in the formation of memory by promoting autophagic flux.
Objectives: To investigate the roles of hippocampal ODC/Spd pathway and autophagic flux in H2S-attenuated cognitive impairment in STZ-induced diabetic rats.
Methods: Cognitive function is judged by the novel objective recognition task (NOR), the Y-maze, and the

Peer review under responsibility of Cairo University.
* Corresponding authorsat: Institute of neurology, The First Affiliated Hospital, University of South China, 69 Chuanshan Road, Hengyang 421001, Hunan, PR China (Xiao-Qing Tang), Department of Neurology, The Second Affiliated Hospital, University of South China, 35 Jiefang Road, Hengyang 421001, Hunan, PR China (Ke-Bin Zhan).
E-mail addresses: zhankb-usc@usc.edu.cn (K.-B. Zhan), tangxq-usc@usc.edu.cn, tangxq-usc@qq.com (X.-Q. Tang).
[1] Xuan Kang and Cheng Li contributed equally to this work.

https://doi.org/10.1016/j.jare.2020.06.007
2090-1232/

Diabetes
Ornithine decarboxylase/spermidine pathway
Hydrogen sulfide

Morris water maze (MWM) tests. The ODC/Spd pathway in hippocampus was evaluated using the expression of ODC detected by western blot and the level of Spd assayed by GC-MS. Autophagic flux was assessed using the expressions of Beclin-1, LC3II/I, and P62 detected by western blot, and the number of autophagosomes observed by transmission electron microscope.

Results: Sodium hydrosulfide (NaHS, a donor of H2S) markedly improved the autophagic flux in the hippocampus of STZ-exposed rats, as evidenced by a decrease in the number of autophagosomes as wells as downregulations in the expressions of LC3-II, Beclin-1, and P62 in the hippocampus of cotreatment with NaHS and STZ rats. NaHS also up-regulated the expression of ODC and the level of Spd in the hippocampus of STZ-induced diabetic rats. Furthermore, inhibited hippocampal ODC/Spd pathway by difluoromethylornithine (DFMO) markedly reversed the protections of NaHS against the hippocampal autophagic flux impairment as well as the cognitive dysfunction in STZ-exposed rats.

Conclusion: These findings indicated that improving hippocampal autophagic flux plays a key role in H2S-attenuated cognitive impairment in STZ-induced diabetic rats, as results of up-regulating hippocampal ODC/Spd pathway.

Introduction

Diabetes mellitus (DM) leads to many serious and debilitating heath complications of multiple organs, such as cardiomyopathy, nephropathy, and retinopathy. Recently, increasing evidence has shown that DM also causes dysfunction of the central nervous system, pathologically characterized by neuron loss and axonal degeneration [1]. Substantial epidemiological evidence supports an association between diabetes and cognitive dysfunction, clinically characterized by chronic progressive varying degrees of cognitive impairment in particular psychomotor slowing and reduced mental flexibility [2]. This phenomenon is termed diabetes-associated cognitive dysfunction (DACD) and has also been confirmed in diabetic animal models. Accumulating evidence has shown that diabetic rodent models presents memory and learning impairments via the impairment of hippocampal neurogenesis [3] and synaptic plasticity [4]. It is therefore of utmost importance to explore novel therapeutic interventions for the treatment of diabetic cognitive dysfunction. Hydrogen sulfide (H_2S), a novel gasotransmitter [5,6], works as a neuroprotectant and neuromodulator [7]. Our previous study has demonstrated that H_2S ameliorates the cognitive dysfunction in STZ-induced diabetic rats [8], opening up a new perspective for the therapeutic intervention of diabetic cognitive dysfunction. However, the underlying mechanisms are still elusive.

Autophagic flux is defined as the flow of autophagosomes from formation to fusion with lysosomes [9]. Previous studies have demonstrated that the autophagic flux in hippocampus of diabetic rats is impaired [10] and that impaired autophagic flux in hippocampus lead to cognitive impairment [11]. Therefore, developing novel therapeutic strategies to enhance hippocampal autophagic flux plays an important role in treatment for the diabetic cognitive impairment. Interestingly, increasing evidence confirms that restoration of autophagic flux contributes to the neuroprotective and cardioprotective effects of H_2S [12,13]. To understand the mechanisms underlying H_2S-attenuated diabetic cognitive dysfunction, we explored whether H_2S enhances the autophagic flux in the hippocampus of diabetic rats.

Polyamines (PAs) play a key role in brain tissues during the early developmental stage, preventing apoptotic neuronal death, and have neuroprotective effects [14–16]. PAs consist of putrescine (Put), spermidine (Spd) and spermine (Spm). The classical polyamines biosynthesis pathway begins with theformation of Put through amino acids ornithine decarboxylate by ornithine decarboxylase (ODC) [17]. Spd and Spm are then formed by adding aminopropyl groups to Put. ODC is the key enzyme of PA biosynthesis [18]. Thus, inhibition of ODC suppresses the production of Spd [17,19]. It has been confirmed that Spd improves memory impairment via enhancing autophagic flux [16,20,21]. Thus, we explored whether ODC/Spd pathway mediates H_2S-ameliorated impairments in cognitive function and hippocampal autophagic flux in STZ-induced diabetic rats.

Our present work showed that H_2S enhanced autophagic flux and up-regulated ODC/Spd pathway in the hippocampus of STZ-induced diabetic rats, and that inhibition of ODC/Spd pathway reversed the improving roles of H_2S in hippocampal autophagic flux and cognitive function in STZ-induced diabetic rats. We, for the first time, demonstrate that hippocampal ODC/Spd pathway through improving hippocampal autophagic flux mediates H_2S-attenuated cognitive impairment in STZ-induced diabetic rats.

Materials and methods

Reagents

NaHS, STZ, and DFMO were obtained from Sigma (Sigma, St. Louis, MO, USA). Specific monoclonal antibody for detecting ODC was supplied by Santa Cruz Biotechnology Inc (Catalog no. : sc-398116, Host: mouse, Delaware Ave Santa Cruz, CA, USA). Specific monoclonal antibodies for detecting Beclin-1 (Catalog no. : 3495 s, Host: rabbit), P62 (Catalog no. : 5114 s, Host: rabbit), and LC3-I/II (Catalog no. : 4108 s, Host: rabbit) were bought from Cell Signaling Technology (Beverly, MA, USA).

Animals

Sprague-Dawley rats (male, 5-week-old, 260–280 g, n = 121) were purchased from the SJA Lab Animal Center of Changsha (Changsha, Hunan, China). The approval number for experimentation with animals is SYXK (Xiang) 2015–0001. The rats were divided into individual cages, housed in temperature at (24 ± 2) °C, with controlled suitable humidity and ventilation. The room was kept in a 12-hours light/dark circle every day. Rats were given ad libitum access to food and water. Experiments were approved by the Animal Use and Protection Committee of University of South China. All efforts were made to minimize injuries.

Drug treatments and experimental schedule

Rats were randomly divided into seven groups: control group (n = 13), daily intraperitoneal (i.p.) injection phosphate-buffered saline (PBS, 1 ml/Kg); STZ-treated alone group (n = 20), which were singly injected with STZ (55 mg/kg, i.p.) and PBS for 30d (1 ml/Kg, i.p.); the co-treatment with STZ and 30 μmol/kg/d NaHS group (n = 20), which received a single injection of STZ (55 mg/kg, i.p.) and NaHS (30 μmol/kg/d, i.p.) for 30 d; the co-treatment with STZ and

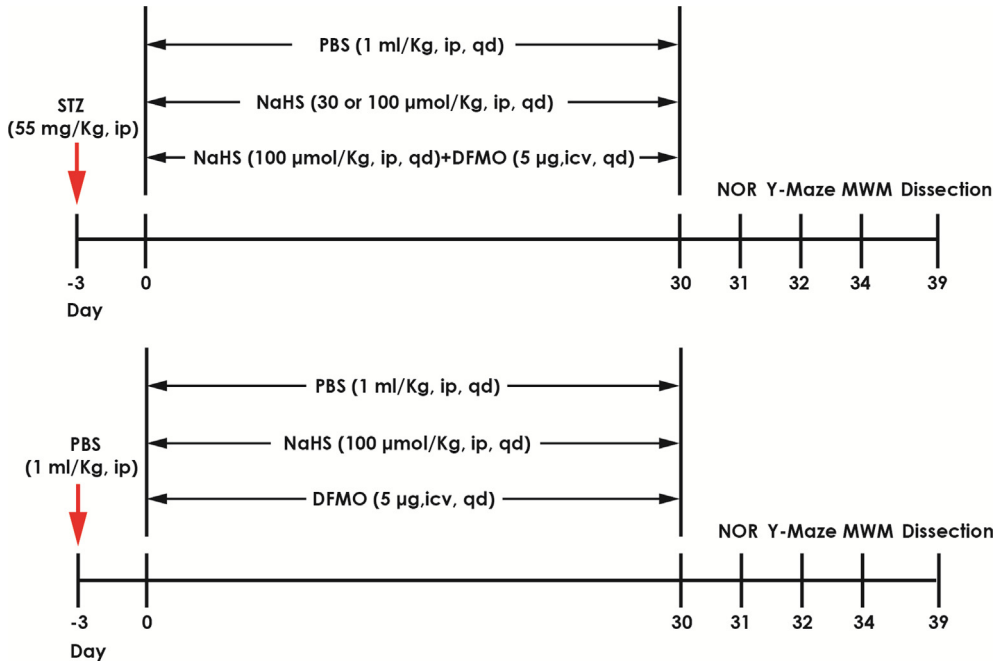

Fig. 1. Experimental time-flow diagram. NOR is short for novel object recognition test. MWM is short for Morris water maze.

100 μmol/kg/d NaHS group (n = 20), which received a single injection of STZ (55 mg/kg, i.p.) and NaHS (100 μmol/kg/d, i.p.) for 30 d; the co-treated with STZ ,100 μmol/kg/d NaHS, and DFMO group (n = 20), which received a single injection of STZ (55 mg/kg, i.p.) and 30-d infusion of NaHS (100 μmol/kg/d, i.p.) as well as intracerebroventricular injection (i.c.v) of DFMO (5 μg/d); 100 μmol/kg/d NaHS-treated alone group (n = 13), which received an intraperitoneal infusion of NaHS (100 μmol/kg/d) for 30 d; and 5 μg/d DFMO-treated alone group (n = 15), which received an intracerebroventricular injection of DFMO (5 μg/d) for 30 d. Behavioral assays to evaluate cognitive level were performed 24 h after the last injection of NaHS and DFMO and within one day after the behavioral tests, rats were sacrificed and the brain tissues were rapidly removed to be stored at −80 °C for analysis (Fig. 1). Meanwhile, the same rats passed all tests during the whole experiment.

Experimental induction of diabetes

Diabetes was induced in rats according to the method described previously [22]. STZ was dissolved in 0.1 M sodium citrate buffer, pH 4.4 and administered at the dose of 55 mg/kg through i.p. route. Four days later, nonfasting blood glucose in a tail-vein sample was determined by a glucose analyzer; a value > 16.7 mmol/L was accepted as a successfully created diabetic model. In the drug administration period, the fasting blood glucose levels were examined every 7 days to make sure fasting blood glucose levels > 16.7 mmol/L.

DFMO administration

DFMO is a dose- and time-dependently enzyme-activated irreversible inhibitor of ODC. DFMO was administered by intracerebroventricular (i.c.v.) injection for 30 days to inhibit hippocampal ODC/Spd activity. After the rats were anesthetized with sodium pentobarbital (50 mg/kg, i.p., Sigma, St. Louis, MO, USA), they were placed into stereotaxic apparatus for orientation at the coordinate (AP: 1.0 mm, R: 2.0 mm, DV: 4.0 mm), and implanted a stainless-steel guide cannula (O.D = 0.64 mm, RWD Life Science Co., Shenzheng, China) into lateral ventricle installed the trocar, affixed to three stainless steel screws. DFMO (5 μg in 2.5 μL) was injected into the ventricle at speed of 0.5 μL/min by using a 5 μL microinjection. Before and after the injection, the needle of microinjection was remained for 1 min in cannula to accommodate injection.

Behavioral procedures

Novel object recognition test

The novel object recognition (NOR) test was used to assess the ability of rats to recognize a novel object in a familiar environment. It included three phases: adaptive (2 days), training and testing phase. In the adaptive phase, every rat was placed in an empty box (50.0 × 50.0 × 60 cm^3) to be adaptive to the environment for 5 min without objects. In the training phase, two identical objects (A and B) were placed in the box, and each rat was allowed to explore them in the box for 5 min. The familiar object exploration time was recorded. One hour after the training phase, the rats entered the test period. In this period, object B was replaced with a novel object C in the box, and each rat was allowed to explore it in the box for another 5 min. The exploration time of novel object was recorded by video-assisted tracking system. The box and the objects were cleaned by 75% alcohol after each test to control the odor cues. Rats climbing or chewing objects was not identified as exploratory behaviors. The cognitive level of rats was analyzed by the discrimination index = (novel object exploration time − same object exploration time)/total exploration time × 100%.

Y-maze test

Y-maze test was also performed to assess the function of learning and memory in rats [23]. Y maze (90 cm length × 90 cm width × 76 cm height) consisted of three black-painted arms (A, B and C) at 120° angles to each other. The rats were habituated in the room for Y-maze test for 30 min. Then each rat was placed in one arm and allowed to move freely in the three arms within 8 min. We recorded the orders and time of rats entering into each arm. If the rats entered three diverse arms in turn, it was regarded as a right alternating sequence. If the rats repeatedly entered the identical arm in three consecutive chances, it was considered as

an incorrect alternating sequence. The total time length of rats entering each arm and the frequency of rats entering correct alternating sequence were recorded to assess the spatial orientation learning ability and activity of the rats. To avoid the effects of smell on the experiment, arms and bottoms were cleaned by 75% alcohol before the experiment.

Morris water maze test

Morris water maze (MWM) test is used to assess the spatial learning and memory and the working memory [24]. The maze is consisted of a 160 cm diameter circular water tank, and equally divided into four quadrants (named 1–4 quadrants). The tank was filled with water up to 30 cm, and the water was rendered opaque by adding milk powder. A transparent escape platform (12-cm diameter, 28-cm height) was placed in the 1st maze quadrants (objective quadrant). Swimming track was recorded by a camera capture, and analyzed by MT-200 Morris image motion system (Chengdu Technology and Market Corp, Chengdu, China). The MWM consisted of training trail, probe trail, and visible platform test. Before the training trial, the rats were habituated in the pool without the platform to assess basal swim speed and spatial bias. In the training trail (the 1st-5th days), each rat was randomly placed to different start locations of the pool for every experiment with the hidden platform being maintained in the same quadrant. Swim track and latency to locate the platform were recorded. Every rat received four training periods per day. In probe trail (the 5th day), the escape platform was removed, and each rat swam freely in the pool for 120 s. The time of the rats staying in the target quadrant and the frequency of the rats crossing target quadrant were recorded and calculated. Visible platform test was used to assess visual and sensorimotor skills after the probe test. In visible platform test, the platform was raised 2 cm above the water surface and moved to novel quadrant. The rats were placed in the opposite side of the platform, and the latency to find the platform as well as the average speed were recorded for calculation.

Spermidine Assay

Hippocampus tissues (weighed 60 g) was homogenized with 500 μL MetOH: H_2O (V : V = 4 : 1) and 20 μL 2-Cl-phenylalanine (0.03 mg/ml) for 2 min using a Tissuelyser-192 homogenizer (Shanghai, China). This homogenate of hippocampus tissue was immediately capped in Vials for extraction at −20 °C for 20 min. The extracted samples were then centrifuged at 14,000 *g* at 4 °C for 10 min and 400 μL of supernatant was transferred to separate vial for GC–MS analysis. The supernatant was evaporated to dryness using a SpeedVac Concentrator System, then subjected to Pyridine hydrochloride solution (15 mg/ml) and vigorously vortex-mixed for 2 min. The supernatant was performed for oximation reaction in oscillation incubator at 37° C for 90 min. And then, 80 μL of N,O-Bis (trimethylsilyl) trifluoroacetamide with 1% Trimethylchlorosilane (BSTFA : TMCS (99:1)) were added and vortex-mixed for 2 min for silylation, and capped in vials and reacted at 70 °C for 1 h. Quality control samples (QC) were prepared by volumes of 25, 50, 100, 250, 500 μL Spd solution (100 μL 1 mg/ml dissolved in 700 μL methyl alcohol). The analysis instrument for this experiment is 7890B-5977A-a gas chromatography mass spectrometry instrument (Agilent, USA). 1ul sample extract after derivatization with no shunt model was sent into GC–MS system for detection, and the sample was separated by nonpolar DB-5 MS capillary column (30 m by 250 mu m I.D., J&W Scientific, Folsom, CA) before into the mass spectrum detection. High purity helium gas is used as carrier gas with gas velocity of 1.0 ml/min. Temperature programmed: 8 °C/min, 80 °C to 100 °C; 10 °C/min, 100 °C to 170 °C; 5 °C/min, 100 °C to 200 °C; 8 °C/ min, 200 °C to 305 °C; 305 °C to maintain 4 min. Injection port of the temperature is 260 °C, EI source temperature is 230 °C, the voltage of −70 V. Quality scan range: *m*/*z* 50–450, delays 5 min to start collection, collection speed of 20 spectra/second.

Observe autophagy by transmission electron microscope

The tissue of hippocampus was separated and cut into 1-mm^3 size samples. The sample was fixed with 2.5% glutaraldehydein for 2 h and with 1% osmic acid for 3 h. After the sample was dehydrated, embedded in paraffin, sliced, and stained with 3% uranyl acetate and lead citrate, autophagy was observed by transmission electron microscope (TEM, JEOL JEM1230, Japan).

SDS-PAGE and western blot

The expressions of LC3-I/II, Beclin-1, P62, and ODC were measured by western blot. After sacrificing the rats, the hippocampal tissues were removed to homogenize with RIPA buffer on the ice. After centrifugation at 12,000 × g for 10 min at 4 °C, the liquid supernatant was then collected, subsequently quantified by using BCA™ Protein Assay Kit (Beyotime, Shanghai, China). Equal quantities of total protein (50 μg/lane) were electrophoresed through 12% sodium dodecyl sulfate–polyacrylamide gel, then wet electrotransferred to polyvinylidene fluoride (PVDF). The membranes were blocked with 5% milk in tris-buffered saline (TBS-T,150 mM NaCl, 0.1% Tween 20, 20 mM tris, pH 7.4) at room temperature for 2 h, then incubated with primary antibodies including monoclonal antibody for LC3 I/II, Beclin-1, P62, and ODC (diluted 1:1,000) or β-actin (1:2,000) at 4 °C overnight. After being washed with TBS-T for three times, the membranes were incubated in corresponding secondary antibody horseradish peroxidase (HRP)-conjugated Goat anti-rabbit or Goat anti-mouse (1:5,000) in TBS-T with 5% milk for 2 h at room temperature. The membranes were then washed again and visualized by an enhanced chemiluminescence kit (Millipore Corporation, Billerica, MA, USA). Images were captured by chemiluminescent imaging system (Tanon 5200 Multi, Shanghai, China) and the integrated optical density for the protein band was analyzed by Image-J software.

Statistical analysis

Data were expressed as mean ± S.E.M. Between-group effects on escape latency in the MWM task was analyzed by repeated measures and multivariate analysis of variance (ANOVA). The significance of differences between other parameters was assessed by one-way ANOVA, LSD-t was applied to the analysis of variance and multiple comparisons between groups. Differences were considered statistically significant at $P < 0.05$.

Result

NaHS attenuates hippocampal impaired autophagic flux in STZ-induced diabetic rats

To explore whether enhancing hippocampal autophagic flux is involved in H_2S-improved cognitive function of STZ-induced diabetic rats, we investigated the effect of H_2S on the autophagic flux in the hippocampus of STZ-induced diabetic rats. As shown in Fig. 2A, the number of autophagosomes ($F_{(4,\ 10)} = 14.790$, $P = 0.0003$) was markedly elevated in the hippocampus of STZ-induced diabetic rats, which significantly decreased by treatment with NaHS (100 μmol/Kg). Furthermore, the expressions of LC3-II/I ($F_{(4,\ 10)} = 5.571$, $P = 0.0127$) (Fig. 2B), Beclin-1 ($F_{(4,\ 10)} = 10.190$, $P = 0.0015$) (Fig. 2C), and p62 ($F_{(4,\ 10)} = 8.058$, $P = 0.0036$) (Fig. 2D) were significantly up-regulated in the hip-

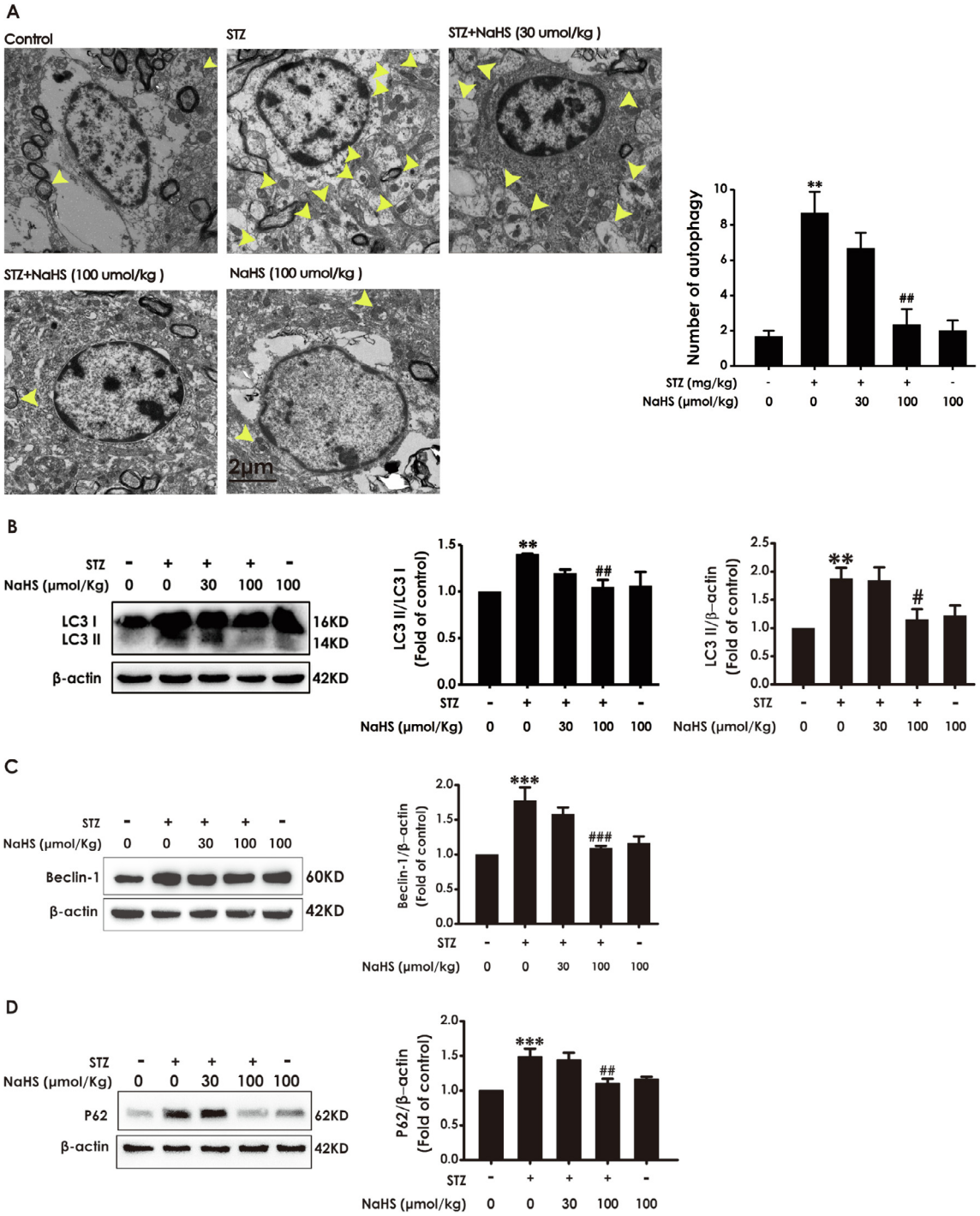

Fig. 2. Effect of NaHS on the hippocampal autophagic flux of STZ-induced diabetic rats. A, The number of autophagosomes in the hippocampus was detected by TEM (Yellow arrows illustrated autophagosomes). B-D, Expressions of LC3-II/I (B), Beclin-1 (C), and P62 (D) in the hippocampus were detected by Western blot using anti-LC3, -Beclin-1, and -P62 antibody, respectively. β-actin was used as loading control. Values are means ± SEM, n = 3. $^{***}P < 0.001$, $^{**}P < 0.01$, *vs* control group; $^{###}P < 0.001$, $^{##}P < 0.01$, $^{#}P < 0.05$, *vs* STZ group.

pocampus of STZ-induced diabetic rats, which also were significantly reversed by treatment with NaHS (100 μmol/Kg). These data indicated that the autophagic flux was blocked in the hippocampus of STZ-induced diabetic rats, which was reversed by treatment with NaHS and suggested the involvement of enhancing hippocampal autophagic flux in the improving role of H_2S in the cognitive function of STZ-induced diabetic rats.

NaHS upregulates hippocampal ODC/Spd pathway in the STZ-induced diabetic rats

To explore the mediatory role of hippocampal ODC/Spd pathway in H_2S-improved cognitive function of STZ-induced diabetic rats, we first investigated the effect of NaHS on the hippocampal ODC/Spd pathway in STZ-induced diabetic rats. The expression of

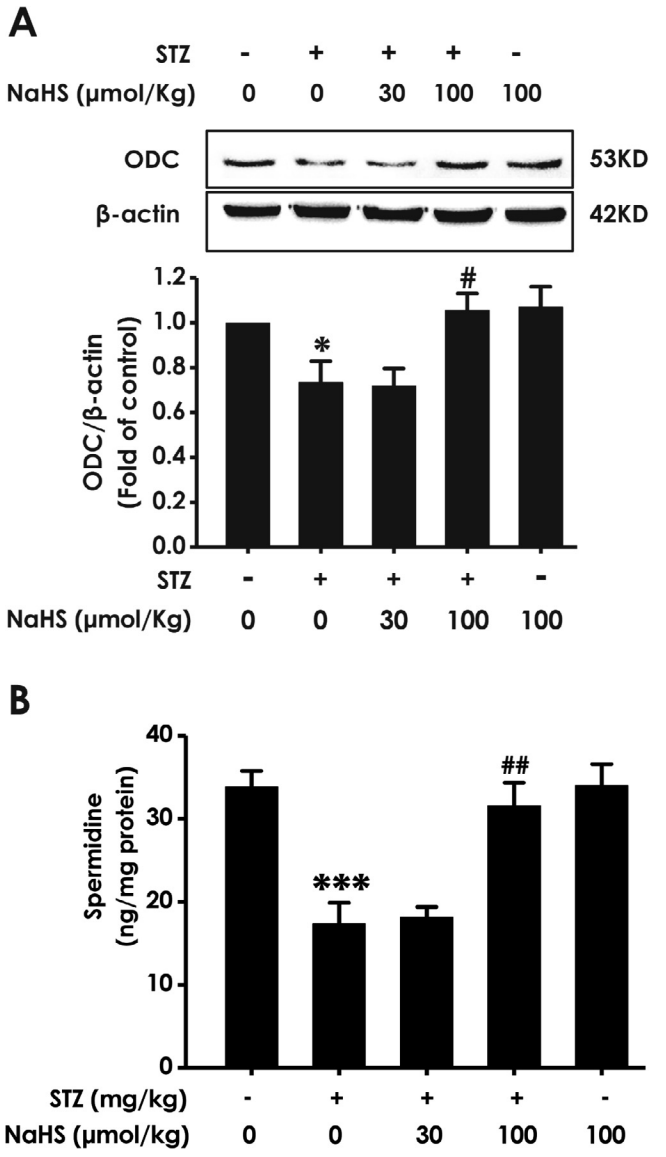

Fig. 3. Effects of NaHS on the ODC/Spd pathway in the hippocampus of STZ-exposed rats. A, Expression of ODC was tested by western blot using anti-ODC antibody. B, The level of Spd in the hippocampus was detected by GC–MS. Values are means ± SEM. n = 3. $^{***}P < 0.001$, $^{*}P < 0.05$, *vs* control group; $^{\#\#}P < 0.01$, $^{\#}P < 0.05$, *vs* STZ group.

ODC ($F_{(4, 10)} = 4.738$, $P = 0.021$) (Fig. 3A) and the level of Spd ($F_{(4, 10)} = 14.019$, $P = 0.0004$) (Fig. 3B) were decreased in the hippocampus of STZ-induced diabetic rats. However, after treatment with NaHS (100 μmol/Kg), the expression of ODC ($F_{(4, 10)} = 4.738$, $P = 0.021$) (Fig. 3A) and the level of Spd ($F_{(4, 10)} = 14.019$, $P = 0.0004$) (Fig. 3B) in the hippocampus of STZ-induced diabetic rats were increased. Our data indicate that NaHS up-regulates the ODC/Spd pathway in the hippocampus of STZ-induced diabetic rats.

DFMO blocks NaHS-increased hippocampal spermidine (Spd) in the STZ-induced diabetic rats

We tested whether DFMO, the inhibitor of ODC, blocks NaHS-increased hippocampal Spd in STZ-exposed rats. As shown in Fig. 4, DFMO (5 μg) markedly decreased the level of Spd ($F_{(4, 10)} = 15.369$, $P = 0.0002$) in the hippocampus of rats cotreated with

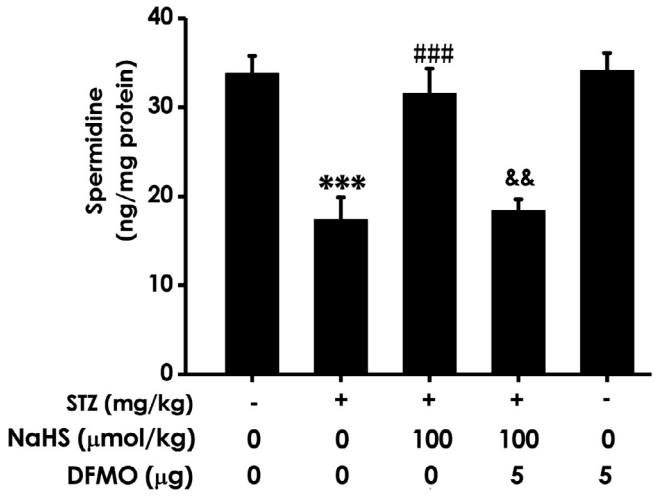

Fig. 4. Effects of DFMO on NaHS-increased the level of Spd in the hippocampus of STZ-exposed rats. The level of Spd in the hippocampus was detected by GC–MS. Values are means ± SEM, n = 3. $^{***}P < 0.001$, *vs* control group; $^{\#\#\#}P < 0.001$, *vs* STZ group; $^{\&\&}P < 0.01$, *vs* NaHS and STZ cotreated group.

NaHS and STZ, which indicate that DFMO blocks the ODC/Spd pathway in the hippocampus of rats cotreated with NaHS and STZ.

DFMO reverses NaHS-attenuated cognitive impairment in STZ-induced diabetic rats

To investigate the mediatory role of hippocampal ODC/Spd pathway in NaHS-attenuated cognitive impairment in STZ-induced diabetic rats, we further explored whether DFMO alters the improving role of H_2S in the cognitive function of STZ-exposed rats using the NOR, Y-maze, and MWM tests.

In the NOR test, NaHS (100 μmol/Kg) significantly increased the discrimination index of STZ-induced diabetic rats; however, DFMO (5 μg) significantly decreased the discrimination index of rats cotreated with NaHS and STZ ($F_{(4, 36)} = 11.030$, $P < 0.0001$) (Fig. 5A). Furthermore, there was no difference in the total amounts of exploration time among the five groups ($F_{(4, 36)} = 1.773$, $P = 0.1558$) (Fig. 5B). These findings revealed that inhibited hippocampal ODC/Spd pathway reverses NaHS-attenuated cognitive impairment in STZ-induced diabetic rats.

In Y-maze test, treatment with NaHS (100 μmol/Kg) ascended the correct rate in STZ-exposed rats, which was reversed by cotreatment with DFMO (5 μg) ($F_{(4, 37)} = 7.185$, $P = 0.0002$) (Fig. 5C), while the total number of entries had no difference among the five groups ($F_{(4, 37)} = 0.465$, $P = 0.761$) (Fig. 5D). These data also indicated that inhibited hippocampal ODC/Spd pathway reverses NaHS-improved working memory in STZ-induced diabetic rats.

We further exlpored the effect of DFMO on the improving role of NaHS in the cognitive function of STZ-treated rats using the MWM test. In the 5th day of acquisition phase, NaHS (100 μmol/Kg) simplified the swimming routes (Fig. 5E) and shortened the escape latency to the hidden platform in STZ-exposed rats ($F_{(4, 28)} = 3.053$, $P = 0.033$) (Fig. 5F), which were significantly reversed by cotreatment with DFMO (5 μg), indicating that DFMO prevents NaHS-improved spatial learning in STZ-exposed rats. In the probe trial, NaHS (100 μmol/Kg) increased the proportionality of swimming time in target quadrant ($F_{(4, 35)} = 5.368$, $P = 0.0018$) (Fig. 5G) and the times of crossing platform ($F_{(4, 35)} = 4.303$, $P = 0.0062$) (Fig. 5H) in STZ-treated rats, which were markedly reversed by cotreatment with DFMO (5 μg), indicating that DFMO abolishes NaHS-improved spatial memory of STZ-exposed rats. In order to rule out the possibility of the alterations of vision and

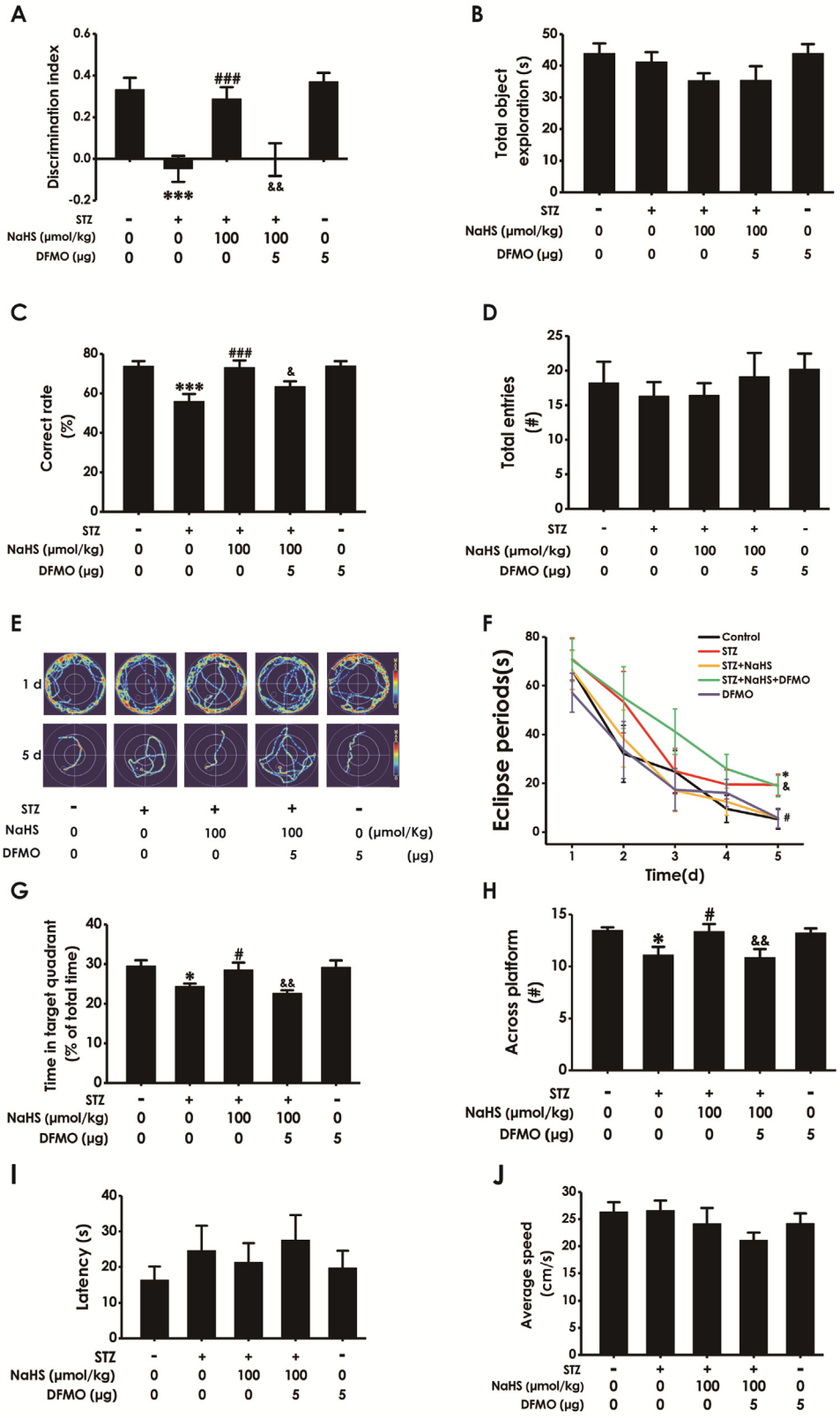

Fig. 5. Effect of DFMO on NaHS-improved cognitive function in STZ-induced diabetic rats. After once injected with STZ (55 mg/kg, i.p.), the rats were treated with NaHS (100 μmol/kg/d, i.p.) and DFMO (5 μg/d, i.p.) for 30 days. A-B, in the Novel object recognition test, the discrimination index (A) and total object exploration (B) were recorded. C-D, in the Y-maze test, the correct rate (C) and total entries number (D) were recorded. E-J, Morris water maze test was used to detect the ability of spatial learning and memory. E-F, in the acquisition phase, the swimming tracks of rats finding for the underwater platform at the 1st and 5th training days (E), the latency to find the underwater platform during 5 days (F) were recorded. G-H, in the probe trail test, the percentage of time in target quadrant (G) and the number of times that the rats crossed the platform (H) were recorded. I-J, in the visible platform test, the latency to reach the platform (I) and the average speed of rats (J) were recorded. Values are means ± SEM, (n = 6–9). $^{***}P < 0.001$, $^{*}P < 0.05$, *vs* control group; $^{###}P < 0.001$, $^{\#}P < 0.05$, *vs* STZ group; $^{\&\&}P < 0.01$, $^{\&}P < 0.05$ *vs* STZ and NaHS co-treated group.

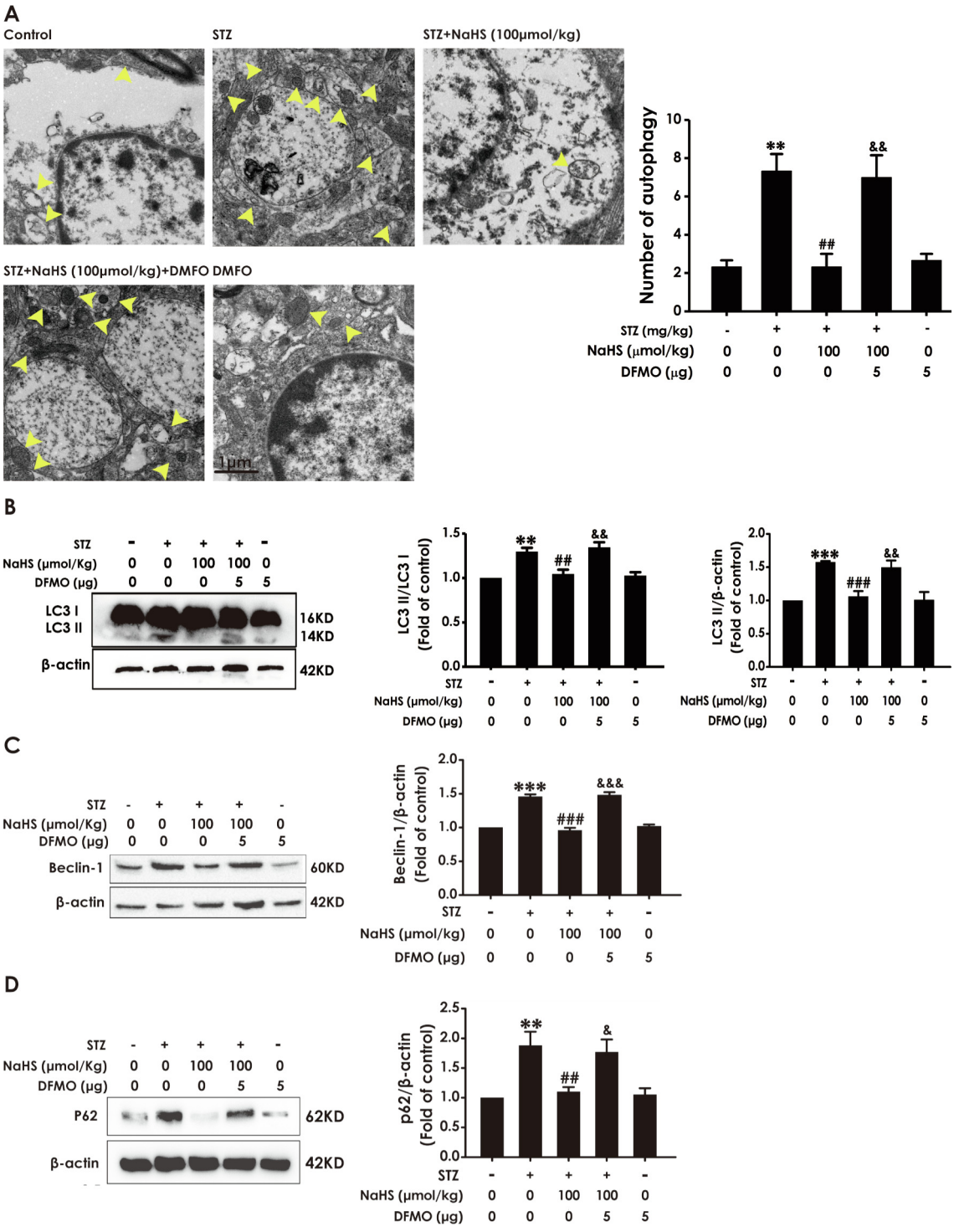

Fig. 6. Effect of DFMO on NaHS-improved hippocampal autophagic flux in STZ-induced diabetic rats. A, The number of autophagosomes in the hippocampus was detected by TEM (Yellow arrows illustrated autophagosomes). B-D, Expressions of LC3-II/I (B), Beclin-1 (C), and P62 (D) in the hippocampus were detected by western blot. Values are means ± SEM, n = 3. $^{***}P < 0.001$, $^{**}P < 0.01$, *vs* control group; $^{\#\#\#}P < 0.001$, $^{\#\#}P < 0.01$, *vs* STZ group; $^{\&\&\&}P < 0.001$, $^{\&\&}P < 0.01$, $^{\&}P < 0.05$ *vs* STZ and NaHS cotreated group.

motor ability, we performed a visible platform test. All groups showed no difference in the latency to the platform ($F_{(4,\ 35)} = 0.572$, $P = 0.6849$) (Fig. 5I) and the average speed ($F_{(4,\ 35)} = 1.209$, $P = 0.324$) (Fig. 5J), which indicated no visual perception and swimming capability change in these experiments. Together, these data from the MWM test also indicated that inhibited hippocampal ODC/Spd pathway reverses NaHS-attenuated cognitive impairment in STZ-induced diabetic rats.

DFMO prevents the improving effect of NaHS on autophagic flux in the hippocampus of STZ-induced diabetic rats

Next, we examined the effect of DFMO on NaHS-improved autophagic flux in the hippocampus of STZ-induced diabetic rats. After treatment with DFMO (5 μg), the number of hippocampal autophagosomes ($F_{(4,\ 10)} = 12.100$, $P = 0.0008$) (Fig. 6A) was increased as well as the expressions of LC3-II/I ($F_{(4,\ 10)} = 12.724$,

$P = 0.0006$) (Fig. 6B), Beclin-1($F_{(4, 10)} = 73.507$, $P < 0.0001$) (Fig. 6C), and p62 ($F_{(4, 10)} = 7.906$, $P = 0.0038$) (Fig. 6D) were up-regulated in the hippocampus of STZ-induced diabetic rats treated with NaHS (100 μmol/Kg), which indicated that inhibited hippocampal ODC/Spd pathway reverses H_2S-improved autophagic flux in STZ-induced diabetic rats.

Discussion

It has been confirmed that ODC/Spd pathway improves memory by enhancing autophagic flux [20] and that impaired hippocampal autophagic flux plays a key role in diabetic cognitive impairment [25]. We have previously demonstrated the improving role of H_2S in the cognitive function of STZ-induced diabetic rats [8]. Based on the regulatory role of H_2S in autophagic flux [26,27], the present work was to investigate the involvement of enhancing hippocampal autophagic flux in H_2S-improved cognitive function in the STZ-exposed rats and the mediatory role of hippocampal ODC/Spd pathway. Our findings are as follows: (1) NaHS up-regulated hippocampal ODC/Spd pathway and enhanced the hippocampal autophagic flux in STZ-induced diabetic rats; (2) Blocked hippocampal ODC/Spd pathway reversed the improving roles of H_2S in the hippocampal autophagic flux and cognitive function of STZ-induced diabetic rats. These results indicated that the improving role of H_2S in the cognitive function of STZ-induced diabetic rats involves enhancement in hippocampal autophagic flux, as a result of up-regulation of hippocampal ODC/Spd pathway.

The rate of diabetes doubled over the past three decades worldwide, and diabetic cognitive impairment increased accordingly [28,29]. Our previous study found that H_2S inhibits the cognitive dysfunction in STZ-induced diabetic rats [8]. A better understanding of why H_2S produces an inhibitory role in diabetic cognitive dysfunction may provide novel information critical for the development of strategy for treatment of diabetic cognitive dysfunction based on H_2S. Diabetes is known to be associated with the damage of hippocampus, which is often believed to be the cause of learning and memory deficits [30,31]. The damage of hippocampus in diabetes is attributed to the impairment in autophagic flux [10,11,32]. Therefore, the present work explored the changes in the hippocampal autophagic flux to reveal the mechanisms underlying the improving role of H_2S in the cognitive function of STZ-induced diabetic rats. Impaired autophagic flux leads to autophagosome accumulation [33–35]. The rising amount of LC3-II/I provides a good index of accumulation of autophagosomes [9]. Beclin-1 is a protein required for the initiation of autophagosome formation and is frequently used as a marker for autophagy [36,37]. P62 is an autophagic cargo protein, which is degraded by lysosomal enzymes and used to determine whether the increase in autophagosomes is due to activation of autophagy or blockade of lysosomal degradation [37,38]. In the present work, we found that the number of autophagosomes corresponded with the levels of LC3-II/I, Beclin-1, and P62 were increased in the hippocampus of STZ-induced diabetic rats, which implied that the fusion of the autophagosomes and lysosomes in the hippocampus of STZ-induced diabetic rats is blocked, meaning that the hippocampal autophagic flux is impaired in the STZ-induced diabetic rats. Notably, treatment with NaHS (100 μmol/Kg) markedly decreased the number of autophagosomes as well as the expressions of LC3-II/I, Beclin-1, and P62 in the hippocampus of STZ-exposed rats, which indicated the improving role of NaHS in the hippocampal autophagic flux of STZ-induced diabetic rats. It has been confirmed that impaired autophagic flux contributes to the pathophysiologic cascade relating with cognitive impairment, while the cognitive impairment is reversed when autophagic flux is restored [25]. Therefore, we suggest that H_2S-improved hippocampal autophagic flux contributes to its inhibitory role in the cognitive dysfunction of STZ-induced diabetic rats.

Spd plays an important role in accelerating the autophagic flux [39,40], resulting in the improvement of learning and memory [41]. Therefore, we explored whether hippocampal ODC/Spd pathway mediates H_2S-improved hippocampal autophagic flux and cognitive function in STZ-exposed rats. We found that the expression of ODC and the level of Spd were decreased in STZ-induced diabetic rats and that treatment of NaHS increased the expression of ODC and the level of Spd in STZ-induced diabetic rats, which indicated that NaHS up-regulates the pathway of ODC/Spd in the hippocampus of STZ-induced diabetic rats. DFMO is an irreversible inhibitor of ODC [18], and we found that DFMO prevented NaHS-increased the level of Spd in the hippocampus of STZ-exposed rats, validating that DFMO prevents the up-regulatory role of NaHS in the hippocampal ODC/Spd pathway of STZ-exposed rats. Furthermore, we also found that DFMO increased the number of autophagosomes as well as the levels of LC3-II, Beclin-1, and P62 in the hippocampus of rats cotreated with NaHS and STZ. These results revealed that the hippocampal ODC/Spd pathway mediates the improving role of H_2S in the hippocampal autophagic flux of STZ-exposed rats.

To investigate whether the ODC/Spd pathway is the underlying mechanism of NaHS-enhanced autophagic flux to inhibit cognitive impairment in the STZ-exposed rats, we explored the effect of DFMO on the improving role of H_2S in the cognitive function of STZ-exposed rats. In present study, the NOR, Y-maze, and MWM tests demonstrate that DFMO prevents NaHS from attenuating the cognitive impairment in the STZ-exposed rats, which indicates that ODC/Spd pathway mediates the improving role of H_2S in the cognitive function of STZ-induced diabetic rats. It has been confirmed that Spd improves learning and memory by enhancement in autophagic flux [41]. Therefore, these results suggest that the improving role of H_2S in the cognitive function of STZ-induced diabetic rats is mediated by upregulation of hippocampal ODC/Spd pathway, which in turn improves the hippocampal autophagic flux.

Conclusion

In conclusion, we demonstrated that NaHS restored the autophagic flux and up-regulated the ODC/Spd pathway in the hippocampus of STZ-induced diabetic rats. Futhermore, blocking hippocampal ODC/Spd pathway reversed the protective roles of NaHS against the hippocampal autophagic flux impairment and the cognitive dysfunction in STZ-induced diabetic rats. Our data revealed that up-regulation of hippocampal ODC/Spd pathway, which in turn enhances hippocampal autophagic flux, plays a critical role in the improving effect of H_2S on the cognitive function of STZ-induced diabetic rats. These findings offer novel insights into the mechanisms underlying the inhibitory role of H_2S in the cognitive impairment of STZ-induced diabetic rats and highlight a promising therapeutic strategy for the diabetic cognitive dysfunction.

Compliance with Ethics Requirements

All Institutional and National Guidelines for the care and use of animals (fisheries) were followed.

Declaration of Competing Interest

The authors declare that they have no known competing financial interests or personal relationships that could have appeared to influence the work reported in this paper.

Acknowledgements

This study is supported by National Natural Science Foundation of China (81671057) and Natural Science Foundation of Hunan province (2019JJ50546, 2019JJ80101, 2019JJ50556).

Xiao-Qing Tang contributed conception and design of the study. Xuan Kang, Cheng Li, Yan Xie and Ling-Li He performed these experiments. Fan Xiao, Yi-Yun Tang, Xiang Li and Ke-Bin Zhan analyzed the data of these experiments. Xuan Kang and Cheng Li wrote this manuscript. Xiao-Qing Tang and Ke-Bin Zhan revised this manuscript. All authors contributed to manuscript revision, read and approved the submitted version.

References

[1] McCrimmon RJ, Ryan CM, Frier BM. Diabetes and cognitive dysfunction. Lancet 2012;379(9833):2291–9.
[2] Koekkoek PS, Kappelle LJ, van den Berg E, Rutten GEHM, Biessels GJ. Cognitive function in patients with diabetes mellitus: guidance for daily care. Lancet Neurol 2015;14(3):329–40.
[3] Ho N, Sommers MS, Lucki I. Effects of diabetes on hippocampal neurogenesis: Links to cognition and depression. Neurosci Biobehav Rev 2013;37 (8):1346–62.
[4] Biessels GJ, Despa F. Cognitive decline and dementia in diabetes mellitus: mechanisms and clinical implications. Nat Rev Endocrinol 2018;14 (10):591–604.
[5] Goodwin LR, Francom D, Dieken FP, Taylor JD, Warenycia MW, Reiffenstein RJ, et al. Determination of Sulfide in Brain Tissue by Gas Dialysis/Ion Chromatography: Postmortem Studies and Two Case Reports. J Anal Toxicol 1989;13(2):105–9.
[6] Warenycia MW, Goodwin LR, Benishin CG, Reiffenstein RJ, Francom DM, Taylor JD, et al. Acute hydrogen sulfide poisoning. Biochem Pharmacol 1989;38 (6):973–81.
[7] Abe K, Kimura H. The possible role of hydrogen sulfide as an endogenous neuromodulator. J Neurosci 1996;16(3):1066–71.
[8] Zou W, Yuan J, Tang ZJ, Wei HJ, Zhu WW, Zhang P, et al. Hydrogen sulfide ameliorates cognitive dysfunction in streptozotocin-induced diabetic rats: involving suppression in hippocampal endoplasmic reticulum stress. Oncotarget 2017;8(38):64203–16.
[9] Lim J, Lee Y, Jung S, Youdim MB, Oh YJ. Impaired autophagic flux is critically involved in drug-induced dopaminergic neuronal death. Parkinsonism & Relat Disord 2014;20:S162–6.
[10] Ma LY, Lv YL, Huo K, Liu J, Shang SH, Fei YL, et al. Autophagy-lysosome dysfunction is involved in Abeta deposition in STZ-induced diabetic rats. Behav Brain Res 2017;320:484–93.
[11] Guan ZF, Zhou XL, Zhang XM, Zhang Y, Wang YM, Guo QL, et al. Beclin-1-mediated autophagy may be involved in the elderly cognitive and affective disorders in streptozotocin-induced diabetic mice. Transl Neurodegener 2016;5:22.
[12] Xie H, Xu Q, Jia J, Ao G, Sun Y, Hu L, et al. Hydrogen sulfide protects against myocardial ischemia and reperfusion injury by activating AMP-activated protein kinase to restore autophagic flux. Biochem Biophys Res Commun 2015;458(3):632–8.
[13] Zhu Y, Shui M, Liu X, Hu W, Wang Y. Increased autophagic degradation contributes to the neuroprotection of hydrogen sulfide against cerebral ischemia/reperfusion injury. Metab Brain Dis 2017;32(5):1449–58.
[14] Harada J, Sugimoto M. Polyamines prevent apoptotic cell death in cultured cerebellar granule neurons. Brain Res 1997;753(2):251–9.
[15] Bell MR, Belarde JA, Johnson HF, Aizenman CD. A neuroprotective role for polyamines in a Xenopus tadpole model of epilepsy. Nat Neurosci 2011;14 (4):505–12.
[16] Fan J, Yang X, Li J, Shu Z, Dai J, Liu X, et al. Spermidine coupled with exercise rescues skeletal muscle atrophy from D-gal-induced aging rats through enhanced autophagy and reduced apoptosis via AMPK-FOXO3a signal pathway. Oncotarget 2017;8(11):17475–90.
[17] Wallace HM, Fraser AV, Hughes A. A perspective of polyamine metabolism. Biochem J 2003;376(1):1–14.
[18] Slotkin TA, Bartolome J. Role of ornithine decarboxylase and the polyamines in nervous system development: A review. Brain Res Bull 1986;17(3):307–20.
[19] Miller-Fleming L, Olin-Sandoval V, Campbell K, Ralser M. Remaining Mysteries of Molecular Biology: The Role of Polyamines in the Cell. J Mol Biol 2015;427 (21):3389–406.
[20] Gupta VK, Scheunemann L, Eisenberg T, Mertel S, Bhukel A, Koemans TS, et al. Restoring polyamines protects from age-induced memory impairment in an autophagy-dependent manner. Nat Neurosci 2013;16(10):1453–60.
[21] Yang Y, Chen S, Zhang Y, Lin X, Song Y, Xue Z, et al. Induction of autophagy by spermidine is neuroprotective via inhibition of caspase 3-mediated Beclin 1 cleavage e2738–e2738. Cell Death Dis 2017;8(4):e2738.
[22] Mehrabani M, Najafi M, Kamarul T, Mansouri K, Iranpour M, Nematollahi MH, et al. Deferoxamine preconditioning to restore impaired HIF-1alpha-mediated angiogenic mechanisms in adipose-derived stem cells from STZ-induced type 1 diabetic rats. Cell Prolif 2015;48(5):532–49.
[23] Cai ZL, Wang CY, Jiang ZJ, Li HH, Liu WX, Gong LW, et al. Effects of cordycepin on Y-maze learning task in mice. Eur J Pharmacol 2013;714(1–3):249–53.
[24] Vorhees CV, Williams MT. Morris water maze: procedures for assessing spatial and related forms of learning and memory. Nat Protoc 2006;1(2):848–58.
[25] Gu HF, Nie YX, Tong QZ, Tang YL, Zeng Y, Jing KQ, et al. Epigallocatechin-3-Gallate Attenuates Impairment of Learning and Memory in Chronic Unpredictable Mild Stress-Treated Rats by Restoring Hippocampal Autophagic Flux. PLoS ONE 2004;9(11):e112683.
[26] Li L, Xiao T, Li F, Li Y, Zeng O, Liu M, et al. Hydrogen sulfide reduced renal tissue fibrosis by regulating autophagy in diabetic rats. Mol Med Rep 2017;16 (2):1715–22.
[27] Wang SS, Chen YH, Chen N, Wang LJ, Chen DX, Weng HL, et al. Hydrogen sulfide promotes autophagy of hepatocellular carcinoma cells through the PI3K/Akt/mTOR signaling pathway. Cell Death Dis 2017;8(3):e2688.
[28] Hamed SA. Brain injury with diabetes mellitus: evidence, mechanisms and treatment implications. Expert Rev Clin Pharmacol 2017;10(4):409–28.
[29] Ingelfinger JR, Jarcho JA. Increase in the Incidence of Diabetes and Its Implications. N Engl J Med 2017;376(15):1473–4.
[30] Xue H, Wang J, Zhuang Y, Gao G. Hippocampal neuron damage and cognitive dysfunction of diabetic Wistar rats. Sheng Wu Yi Xue Gong Cheng Xue Za Zhi 2014;31(6):1305–9.
[31] Ni B, Wu R, Yu T, Zhu H, Li Y, Liu Z. Role of the Hippocampus in Distinct Memory Traces: Timing of Match and Mismatch Enhancement Revealed by Intracranial Recording. Neurosci Bull 2017;33(6):664–74.
[32] Dhikav V, Anand K. Potential predictors of hippocampal atrophy in Alzheimer's disease. Drugs Aging 2011;28(1):1–11.
[33] Mizushima N, Yoshimori T, Levine B. Methods in Mammalian Autophagy Research. Cell 2010;140(3):313–26.
[34] Gonzalez CD, Lee MS, Marchetti P, Pietropaolo M, Towns R, Vaccaro MI, et al. The emerging role of autophagy in the pathophysiology of diabetes mellitus. Autophagy 2011;7(1):2–11.
[35] Sarkar C, Zhao Z, Aungst S, Sabirzhanov B, Faden AI, Lipinski MM. Impaired autophagy flux is associated with neuronal cell death after traumatic brain injury. Autophagy 2014;10(12):2208–22.
[36] Kimura S, Fujita N, Noda T, Yoshimori T. Monitoring autophagy in mammalian cultured cells through the dynamics of LC3. Methods Enzymol 2009;452:1–12.
[37] Klionsky DJ, Abdalla FC, Abeliovich H, Abraham RT, Acevedo-Arozena A, Adeli K, et al. Guidelines for the use and interpretation of assays for monitoring autophagy. Autophagy 2012;8(4):445–544.
[38] Ulland TK, Song WM, Huang SC, Ulrich JD, Sergushichev A, Beatty WL, et al. TREM2 Maintains Microglial Metabolic Fitness in Alzheimer's Disease. Cell 2017;170(4):649–663.e13.
[39] Bhukel A, Madeo F, Sigrist SJ. Spermidine boosts autophagy to protect from synapse aging. Autophagy 2017;13(2):444–5.
[40] Tong D, Hill JA. Spermidine Promotes Cardioprotective Autophagy. Circ Res 2017;120(8):1229–31.
[41] Sigrist SJ, Carmona-Gutierrez D, Gupta VK, Bhukel A, Mertel S, Eisenberg T, et al. Spermidine-triggered autophagy ameliorates memory during aging. Autophagy 2014;10(1):178–9.